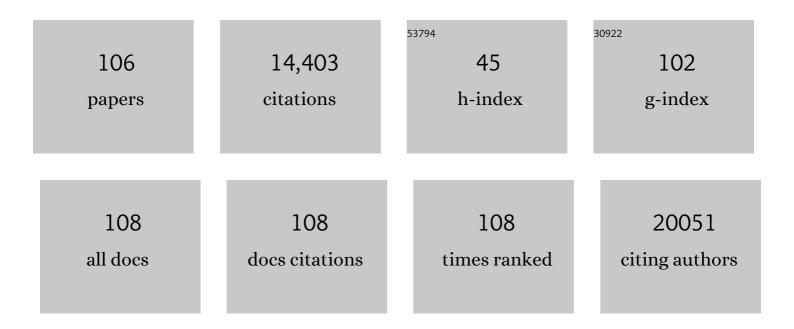
## Ki Kang Kim

List of Publications by Year in descending order

Source: https://exaly.com/author-pdf/7664066/publications.pdf Version: 2024-02-01



#	Article	IF	CITATIONS
1	Efficient Reduction of Graphite Oxide by Sodium Borohydride and Its Effect on Electrical Conductance. Advanced Functional Materials, 2009, 19, 1987-1992.	14.9	2,059
2	Synthesis of Few-Layer Hexagonal Boron Nitride Thin Film by Chemical Vapor Deposition. Nano Letters, 2010, 10, 4134-4139.	9.1	1,058
3	Synthesis of Monolayer Hexagonal Boron Nitride on Cu Foil Using Chemical Vapor Deposition. Nano Letters, 2012, 12, 161-166.	9.1	1,057
4	van der Waals Epitaxy of MoS <sub>2</sub> Layers Using Graphene As Growth Templates. Nano Letters, 2012, 12, 2784-2791.	9.1	888
5	Effect of Acid Treatment on Carbon Nanotube-Based Flexible Transparent Conducting Films. Journal of the American Chemical Society, 2007, 129, 7758-7759.	13.7	874
6	Synthesis of Largeâ€Area Graphene Layers on Polyâ€Nickel Substrate by Chemical Vapor Deposition: Wrinkle Formation. Advanced Materials, 2009, 21, 2328-2333.	21.0	814
7	Work Function Engineering of Graphene Electrode <i>via</i> Chemical Doping. ACS Nano, 2010, 4, 2689-2694.	14.6	501
8	Synthesis and Characterization of Hexagonal Boron Nitride Film as a Dielectric Layer for Graphene Devices. ACS Nano, 2012, 6, 8583-8590.	14.6	472
9	Understanding and controlling the substrate effect on graphene electron-transfer chemistry via reactivity imprint lithography. Nature Chemistry, 2012, 4, 724-732.	13.6	463
10	Synthesis of large-area multilayer hexagonal boron nitride for high material performance. Nature Communications, 2015, 6, 8662.	12.8	403
11	Wafer-scale single-crystal hexagonal boron nitride film via self-collimated grain formation. Science, 2018, 362, 817-821.	12.6	336
12	Enhancing the conductivity of transparent graphene films via doping. Nanotechnology, 2010, 21, 285205.	2.6	321
13	Doped graphene electrodes for organic solar cells. Nanotechnology, 2010, 21, 505204.	2.6	241
14	Fermi Level Engineering of Single-Walled Carbon Nanotubes by AuCl <sub>3</sub> Doping. Journal of the American Chemical Society, 2008, 130, 12757-12761.	13.7	238
15	Phase-Engineered Synthesis of Centimeter-Scale 1T′- and 2H-Molybdenum Ditelluride Thin Films. ACS Nano, 2015, 9, 6548-6554.	14.6	225
16	Biexciton Emission from Edges and Grain Boundaries of Triangular WS <sub>2</sub> Monolayers. ACS Nano, 2016, 10, 2399-2405.	14.6	220
17	Anisotropic electrical conductivity of MWCNT/PAN nanofiber paper. Chemical Physics Letters, 2005, 413, 188-193.	2.6	202
18	Large-Area Monolayer Hexagonal Boron Nitride on Pt Foil. ACS Nano, 2014, 8, 8520-8528.	14.6	200

Ki Kang Kim

#	Article	IF	CITATIONS
19	Reduction-Controlled Viologen in Bisolvent as an Environmentally Stable n-Type Dopant for Carbon Nanotubes. Journal of the American Chemical Society, 2009, 131, 327-331.	13.7	196
20	Synthesis of Patched or Stacked Graphene and hBN Flakes: A Route to Hybrid Structure Discovery. Nano Letters, 2013, 13, 933-941.	9.1	179
21	Tailoring Electronic Structures of Carbon Nanotubes by Solvent with Electron-Donating and -Withdrawing Groups. Journal of the American Chemical Society, 2008, 130, 2062-2066.	13.7	178
22	Synthesis of Centimeter-Scale Monolayer Tungsten Disulfide Film on Gold Foils. ACS Nano, 2015, 9, 5510-5519.	14.6	166
23	Role of Anions in the AuCl <sub>3</sub> -Doping of Carbon Nanotubes. ACS Nano, 2011, 5, 1236-1242.	14.6	149
24	Doping and de-doping of carbon nanotube transparent conducting films by dispersant and chemical treatment. Journal of Materials Chemistry, 2008, 18, 1261.	6.7	132
25	Impact of Graphene Interface Quality on Contact Resistance and RF Device Performance. IEEE Electron Device Letters, 2011, 32, 1008-1010.	3.9	126
26	Absorption spectroscopy of surfactant-dispersed carbon nanotube film: Modulation of electronic structures. Chemical Physics Letters, 2008, 455, 275-278.	2.6	124
27	Large-scale synthesis of graphene and other 2D materials towards industrialization. Nature Communications, 2022, 13, 1484.	12.8	123
28	The effect of copper pre-cleaning on graphene synthesis. Nanotechnology, 2013, 24, 365602.	2.6	122
29	Optical absorption spectroscopy for determining carbon nanotube concentration in solution. Synthetic Metals, 2007, 157, 570-574.	3.9	120
30	Photocatalytic improvement of Mn-adsorbed g-C3N4. Applied Catalysis B: Environmental, 2017, 206, 271-281.	20.2	118
31	Synthesis of hexagonal boron nitride heterostructures for 2D van der Waals electronics. Chemical Society Reviews, 2018, 47, 6342-6369.	38.1	114
32	Controlling work function of reduced graphite oxide with Au-ion concentration. Chemical Physics Letters, 2009, 475, 91-95.	2.6	104
33	Semiconductor–Insulator–Semiconductor Diode Consisting of Monolayer MoS <sub>2</sub> , h-BN, and GaN Heterostructure. ACS Nano, 2015, 9, 10032-10038.	14.6	88
34	Enhancement of Conductivity by Diameter Control of Polyimide-Based Electrospun Carbon Nanofibers. Journal of Physical Chemistry B, 2007, 111, 11350-11353.	2.6	81
35	Metal–Insulator–Semiconductor Diode Consisting of Two-Dimensional Nanomaterials. Nano Letters, 2016, 16, 1858-1862.	9.1	74
36	High-Yield Catalytic Synthesis of Thin Multiwalled Carbon Nanotubes. Journal of Physical Chemistry B, 2004, 108, 17695-17698.	2.6	71

#	Article	IF	CITATIONS
37	Dependence of Raman spectra <mml:math <br="" xmlns:mml="http://www.w3.org/1998/Math/MathML">display="inline"&gt;<mml:msup><mml:mi>G</mml:mi><mml:mo>′</mml:mo></mml:msup></mml:math> band intensity on metallicity of single-wall carbon nanotubes. Physical Review B, 2007, 76, .	3.2	67
38	Dispersion Stability of Single-Walled Carbon Nanotubes Using Nafion in Bisolvent. Journal of Physical Chemistry C, 2007, 111, 2477-2483.	3.1	66
39	Restoring the photovoltaic effect in graphene-based van der Waals heterojunctions towards self-powered high-detectivity photodetectors. Nano Energy, 2019, 57, 214-221.	16.0	65
40	Characterization of thin multi-walled carbon nanotubes synthesized by catalytic chemical vapor deposition. Chemical Physics Letters, 2005, 413, 135-141.	2.6	63
41	Doping strategy of carbon nanotubes with redox chemistry. New Journal of Chemistry, 2010, 34, 2183.	2.8	63
42	Restorable Type Conversion of Carbon Nanotube Transistor Using Pyrolytically Controlled Antioxidizing Photosynthesis Coenzyme. Advanced Functional Materials, 2009, 19, 2553-2559.	14.9	59
43	Transparent Organic P-Dopant in Carbon Nanotubes: Bis(trifluoromethanesulfonyl)imide. ACS Nano, 2010, 4, 6998-7004.	14.6	56
44	Epitaxial Singleâ€Crystal Growth of Transition Metal Dichalcogenide Monolayers via the Atomic Sawtooth Au Surface. Advanced Materials, 2021, 33, e2006601.	21.0	55
45	A Novel and Facile Route to Synthesize Atomic‣ayered MoS <sub>2</sub> Film for Largeâ€Area Electronics. Small, 2017, 13, 1701306.	10.0	53
46	Tipâ€Induced Nanoâ€Engineering of Strain, Bandgap, and Exciton Funneling in 2D Semiconductors. Advanced Materials, 2021, 33, e2008234.	21.0	44
47	Nanodispersion of Single-Walled Carbon Nanotubes Using Dichloroethane. Journal of Nanoscience and Nanotechnology, 2005, 5, 1055-1059.	0.9	41
48	Modulating Electronic Properties of Monolayer MoS <sub>2</sub> <i>via</i> Electron-Withdrawing Functional Groups of Graphene Oxide. ACS Nano, 2016, 10, 10446-10453.	14.6	41
49	Selective Oxidation on Metallic Carbon Nanotubes by Halogen Oxoanions. Journal of the American Chemical Society, 2008, 130, 2610-2616.	13.7	40
50	Surface-Induced Hybridization between Graphene and Titanium. ACS Nano, 2014, 8, 7704-7713.	14.6	38
51	Exfoliation of Single-Walled Carbon Nanotubes Induced by the Structural Effect of Perylene Derivatives and Their Optoelectronic Properties. Journal of Physical Chemistry C, 2008, 112, 15267-15273.	3.1	35
52	Flexible plane heater: Graphite and carbon nanotube hybrid nanocomposite. Synthetic Metals, 2015, 203, 127-134.	3.9	35
53	Charge transfer in graphene/polymer interfaces for CO2 detection. Nano Research, 2018, 11, 3529-3536.	10.4	34
54	Carbon Nanotube Doping Mechanism in a Salt Solution and Hygroscopic Effect: Density Functional Theory. ACS Nano, 2010, 4, 5430-5436.	14.6	32

#	Article	IF	CITATIONS
55	Chemically Conjugated Carbon Nanotubes and Graphene for Carrier Modulation. Accounts of Chemical Research, 2016, 49, 390-399.	15.6	30
56	Tailoring Domain Morphology in Monolayer NbSe <sub>2</sub> and W <sub><i>x</i></sub> Nb <sub>1–<i>x</i></sub> Se <sub>2</sub> Heterostructure. ACS Nano, 2020, 14, 8784-8792.	14.6	30
57	Synthesis of Large-Area Tungsten Disulfide Films on Pre-Reduced Tungsten Suboxide Substrates. ACS Applied Materials & Interfaces, 2017, 9, 43021-43029.	8.0	29
58	Deep Learningâ€Assisted Quantification of Atomic Dopants and Defects in 2D Materials. Advanced Science, 2021, 8, e2101099.	11.2	29
59	PURITY MEASUREMENT OF SINGLE-WALLED CARBON NANOTUBES BY UV-VIS-NIR ABSORPTION SPECTROSCOPY AND THERMOGRAVIMETRIC ANALYSIS. Nano, 2008, 03, 101-108.	1.0	28
60	A new horizon for hexagonal boron nitride film. Journal of the Korean Physical Society, 2014, 64, 1605-1616.	0.7	28
61	Effect of Carbon Nanotube Types in Fabricating Flexible Transparent Conducting Films. Journal of the Korean Physical Society, 2008, 53, 979-985.	0.7	28
62	Atomic and structural modifications of two-dimensional transition metal dichalcogenides for various advanced applications. Chemical Science, 2022, 13, 7707-7738.	7.4	28
63	Water-Assisted Synthesis of Molybdenum Disulfide Film with Single Organic Liquid Precursor. Scientific Reports, 2017, 7, 1983.	3.3	27
64	Delay Analysis of Graphene Field-Effect Transistors. IEEE Electron Device Letters, 2012, 33, 324-326.	3.9	26
65	Impact of graphene and single-layer BN insertion on bipolar resistive switching characteristics in tungsten oxide resistive memory. Thin Solid Films, 2015, 589, 188-193.	1.8	21
66	Drift-dominant exciton funneling and trion conversion in 2D semiconductors on the nanogap. Science Advances, 2022, 8, eabm5236.	10.3	21
67	Dual quartz crystal microbalance for hydrogen storage in carbon nanotubes. International Journal of Hydrogen Energy, 2007, 32, 3442-3447.	7.1	20
68	Seed Growth of Tungsten Diselenide Nanotubes from Tungsten Oxides. Small, 2015, 11, 2192-2199.	10.0	20
69	Large-Scale Graphene on Hexagonal-BN Hall Elements: Prediction of Sensor Performance without Magnetic Field. ACS Nano, 2016, 10, 8803-8811.	14.6	20
70	Substitutional Vanadium Sulfide Nanodispersed in MoS <sub>2</sub> Film for Pt‣calable Catalyst. Advanced Science, 2021, 8, e2003709.	11.2	19
71	Thickness-controlled multilayer hexagonal boron nitride film prepared by plasma-enhanced chemical vapor deposition. Current Applied Physics, 2016, 16, 1229-1235.	2.4	18
72	One-Dimensional Single-Chain Nb <sub>2</sub> Se <sub>9</sub> as Efficient Electrocatalyst for Hydrogen Evolution Reaction. ACS Applied Energy Materials, 2019, 2, 5785-5792.	5.1	18

Ki Kang Kim

#	Article	IF	CITATIONS
73	Strategy for High Concentration Nanodispersion of Single-Walled Carbon Nanotubes with Diameter Selectivity. Journal of Physical Chemistry C, 2009, 113, 10044-10051.	3.1	17
74	Spectroscopic Determination of the Electrochemical Potentials of n-Type Doped Carbon Nanotubes. Journal of Physical Chemistry C, 2012, 116, 5444-5449.	3.1	17
75	Wafer-Scale van der Waals Heterostructures with Ultraclean Interfaces via the Aid of Viscoelastic Polymer. ACS Applied Materials & Interfaces, 2019, 11, 1579-1586.	8.0	17
76	A systematic study of the synthesis of monolayer tungsten diselenide films on gold foil. Current Applied Physics, 2016, 16, 1216-1222.	2.4	16
77	First-principles calculation the electronic structure and the optical properties of Mn-decorated g-C3N4 for photocatalytic applications. Journal of the Korean Physical Society, 2016, 69, 1445-1449.	0.7	15
78	Opposite Polarity Surface Photovoltage of MoS <sub>2</sub> Monolayers on Au Nanodot versus Nanohole Arrays. ACS Applied Materials & Interfaces, 2020, 12, 48991-48997.	8.0	15
79	Ambient-pressure CVD of graphene on low-index Ni surfaces using methane: A combined experimental and first-principles study. Physical Review Materials, 2018, 2, .	2.4	12
80	Atomistic mechanisms of seeding promoter-controlled growth of molybdenum disulphide. 2D Materials, 2020, 7, 015013.	4.4	11
81	Fluidic Properties of Carbon Nanotube Inks and Field Emission Properties of Ink Jet-Printed Emitters. Japanese Journal of Applied Physics, 2009, 48, 111601.	1.5	9
82	Control of pâ€doping on singleâ€walled carbon nanotubes with nitronium hexafluoroantimonate in liquid phase. Physica Status Solidi (B): Basic Research, 2009, 246, 2419-2422.	1.5	8
83	Alkali Metal-Assisted Growth of Single-Layer Molybdenum Disulfide. Journal of the Korean Physical Society, 2019, 74, 1032-1038.	0.7	8
84	Quantitative insights into the growth mechanisms of nanopores in hexagonal boron nitride. Physical Review Materials, 2020, 4, .	2.4	8
85	Correlation of Defect-Induced Photoluminescence and Raman Scattering in Monolayer WS <sub>2</sub> . Journal of Physical Chemistry C, 2022, 126, 7177-7183.	3.1	8
86	Sequential Growth of Vertical Transition-Metal Dichalcogenide Heterostructures on Rollable Aluminum Foil. ACS Nano, 2022, 16, 8851-8859.	14.6	8
87	Effective characterization of polymer residues on two-dimensional materials by Raman spectroscopy. Nanotechnology, 2015, 26, 485701.	2.6	7
88	Poly(methyl methacrylate)-derived graphene films on different substrates using rapid thermal process: a way to control the film properties through the substrate and polymer layer thickness. Journal of Materials Research and Technology, 2019, 8, 3752-3763.	5.8	7
89	Synthesis of Transition Metal Disulfides with Liquid Ammonium Sulfide as a Reliable Sulfur Precursor. Applied Science and Convergence Technology, 2019, 28, 60-65.	0.9	7
90	Polarization-Dependent Light Emission and Charge Creation in MoS <sub>2</sub> Monolayers on Plasmonic Au Nanogratings. ACS Applied Materials & Interfaces, 2020, 12, 44088-44093.	8.0	6

#	Article	IF	CITATIONS
91	Toward non-gas-permeable hBN film growth on smooth Fe surface. 2D Materials, 2021, 8, 034003.	4.4	5
92	Two-dimensional air-stable CrSe <sub>2</sub> nanosheets with thickness-tunable magnetism. Journal of Semiconductors, 2021, 42, 100401.	3.7	5
93	Exciton Transfer at Heterointerfaces of MoS <sub>2</sub> Monolayers and Fluorescent Molecular Aggregates. Advanced Science, 2022, 9, .	11.2	5
94	Identifying the Origin of Defect-Induced Raman Mode in WS <sub>2</sub> Monolayers via Density Functional Perturbation Theory. Journal of Physical Chemistry C, 2022, 126, 4182-4187.	3.1	4
95	Hydrogen evolution reaction catalyst with high catalytic activity by interplay between organic molecules and transition metal dichalcogenide monolayers. Materials Today Energy, 2022, 25, 100976.	4.7	4
96	Energetic Sulfide Vaporâ€Processed Colloidal InAs Quantum Dot Solids for Efficient Charge Transport and Photoconduction. Advanced Photonics Research, 2022, 3, .	3.6	4
97	Bias-induced doping engineering with ionic adsorbates on single-walled carbon nanotube thin film transistors. New Journal of Physics, 2008, 10, 113013.	2.9	3
98	Anomalous Light-Induced Charging in MoS <sub>2</sub> Monolayers with Cracks. ACS Applied Electronic Materials, 2021, 3, 5265-5271.	4.3	3
99	Graphene electronics for RF applications. , 2011, , .		2
100	Enhanced Electron Heat Conduction in TaS3 1D Metal Wire. Materials, 2021, 14, 4477.	2.9	2
101	Toward Charge Neutralization of CVD Graphene. Applied Science and Convergence Technology, 2015, 24, 268-272.	0.9	2
102	Universal Transfer of 2D Materials Grown on Au Substrate Using Sulfur Intercalation. Applied Science and Convergence Technology, 2021, 30, 45-49.	0.9	1
103	Substitutional Vanadium Sulfide Nanodispersed in MoS <sub>2</sub> Film for Pt calable Catalyst (Adv.) Tj ET	Qq110.7	84314 rgBT
104	Interface Trap Suppression and Electron Doping in Van der Waals Materials Using Cross-Linked Poly(vinylpyrrolidone). ACS Applied Materials & Interfaces, 2021, 13, 55489-55497.	8.0	1
105	Front Cover (Phys. Status Solidi B 11â€12/2009). Physica Status Solidi (B): Basic Research, 2009, 246, .	1.5	0
106	Nanotransistors using graphene interfaced with advanced dielectrics for high speed communication. , 2011, , .		0